

Distinct requirements of linker DNA and transcriptional activators in promoting SAGA-mediated nucleosome acetylation

Received for publication, June 19, 2018, and in revised form, July 20, 2018 Published, Papers in Press, July 27, 2018, DOI 10.1074/jbc.RA118.004487

Chitvan Mittal^{1,2}, Sannie J. Culbertson^{1,3}, and Michael A. Shogren-Knaak⁴

From the Roy J. Carver Department of Biochemistry, Biophysics and Molecular Biology, Iowa State University, Ames, Iowa 50011

Edited by Joel Gottesfeld

The Spt-Ada-Gcn5 acetyltransferase (SAGA) family of transcriptional coactivators are prototypical nucleosome acetyltransferase complexes that regulate multiple steps in gene transcription. The size and complexity of both the SAGA enzyme and the chromatin substrate provide numerous opportunities for regulating the acetylation process. To better probe this regulation, here we developed a bead-based nucleosome acetylation assay to characterize the binding interactions and kinetics of acetylation with different nucleosomal substrates and the full SAGA complex purified from budding yeast (*Saccharomyces cerevisiae*). We found that SAGA-mediated nucleosome acetylation is stimulated up to 9-fold by DNA flanking the nucleosome, both by facilitating the binding of SAGA and by accelerating acetylation turnover. This stimulation required that flanking DNA is present on both sides of the nucleosome and that one side is >15 bp long. The Gal4–VP16 transcriptional activator fusion protein could also augment nucleosome acetylation up to 5-fold. However, contrary to our expectations, this stimulation did not appear to occur by stabilizing the binding of SAGA toward nucleosomes containing an activator-binding site. Instead, increased acetylation turnover by SAGA stimulated nucleosome acetylation. These results suggest that the Gal4–VP16 transcriptional activator directly stimulates acetylation via a dual interaction with both flanking DNA and SAGA. Altogether, these findings uncover several critical mechanisms of SAGA regulation by chromatin substrates.

The Spt-Ada-Gcn5 acetyltransferase (SAGA)⁵ family of transcriptional coactivators are large, multisubunit complexes

that are highly conserved across eukaryotic species, from yeast to humans (1). Subunits of SAGA were originally identified as effectors of transcription through genetic screens in budding yeast (2, 3), and they were later shown to be associated in a complex containing at least 19 different protein subunits (4, 5). In yeast, SAGA has been shown to be important for the transcription of the majority of all inducible genes, such as stress-response genes that account for ~10% of the yeast genome (6). In higher eukaryotes, SAGA not only regulates genes that are expressed in response to external stress, but also those activated by developmental cues (7). Indeed, mice lacking SAGA perish during embryogenesis (8), and defects in SAGA subunits in humans can lead to congenital disorders, such as the neurodegenerative condition of spinocerebellar ataxia type 7 (9, 10). In addition to its role in transcription, SAGA has also been shown to be involved in mRNA export (11), DNA repair (12), and DNA replication (13).

One of the major ways that SAGA achieves its function is through its innate histone acetyltransferase activity. This catalytic activity resides in the Gcn5 subunit of SAGA, which transfers acetyl groups from acetyl-CoA (CoA) to lysine residues in the tails of histone proteins (14). Heterologously expressed Gcn5 acetylates a single lysine residue, Lys-14, on free histone H3 (15). However, when associated with other SAGA subunits, Gcn5 gains additional specificity and acetylates up to six lysine residues on H3 and to a smaller degree on H2B (4, 16–18). During transcription, this histone acetylation generates transcriptionally activated chromatin, and in yeast, SAGA mediates this acetylation in several different ways. Under rich medium conditions, SAGA maintains a basal state of histone acetylation globally throughout the yeast genome, poising genes for activation (19). Under stress conditions, SAGA becomes localized to the promoters of induced genes and acetylates chromatin to facilitate transcription initiation (20). Additionally, for all transcribed genes, SAGA is present in the open reading frames of genes, and histone acetylation assists in transcriptional elongation (21).

How the localization and activity of SAGA are regulated is key to its biological function, and a number of factors have been identified, including the incorporation of histones into nucleosomes (22), post-translational histone modifications (23–25), and SAGA-interacting chromatin-associated proteins (26–28). An important class of SAGA-interacting chromatin-associated proteins are the transcriptional activators (29). These proteins are downstream of signaling pathways and bind

This work was supported in part by American Cancer Society Research Scholar Grant 1206501 (to M. A. S.-K.). The authors declare that they have no conflicts of interest with the contents of this article.

This article was selected as one of our Editors' Picks.

This article contains Fig. S1 and supporting Methods.

¹ Both authors contributed equally to this work.

² Present address: Dept. of Biochemistry and Molecular Biology, Pennsylvania State University, University Park, PA 16802.

³ Supported in part by a Gary Roewe Research Award. Present address: Division of Genetics, Harvard Medical School, Boston, MA 02115.

⁴ To whom correspondence should be addressed. Tel.: 515-294-9015; Fax: 515-294-0453; E-mail: knaak@iastate.edu.

⁵ The abbreviations used are: SAGA, Spt-Ada-Gcn5 acetyltransferase; CoA, coenzyme A; GBY, DNA template with Gal4-binding site and 95 and 15 bp of DNA flanking a 147-bp nucleosome positioning sequence; DNA template with no DNA flanking a 147-bp nucleosome positioning sequence; EMSA, electrophoretic mobility shift assays; TAP, tandem affinity purification; PMSF, phenylmethylsulfonyl fluoride; TBE, Tris/borate/EDTA buffer; TBP, TATA-binding protein.

This is an open access article under the CC BY license.

to promoter regions of induced genes to initiate transcription. In addition to a DNA-binding domain, they contain a transcriptional activation domain that can interact with a number of transcriptional coactivators and general transcription factors (30–32). Yeast SAGA has been shown to directly interact with numerous different transcriptional activator proteins (29), and this interaction stimulates nucleosome acetylation, both *in vivo* and *in vitro* (33–35).

To ultimately better understand the requirements and mechanism of activator-mediated stimulation of SAGA acetylation, we previously developed a nucleosome acetylation assay that utilized chromatin model systems assembled from individual nucleosomes and purified endogenous SAGA complex from budding yeast (36). In the course of developing this assay, we obtained results suggesting that the DNA flanking a nucleosome could stimulate SAGA activity. To substantiate these results, as well as to characterize the effect of activator proteins, here we develop several new assays for characterizing nucleosome acetylation and binding, and we apply them to studying the role of flanking DNA and activator on SAGA-mediated nucleosome acetylation.

Results

SAGA-mediated nucleosome acetylation

To characterize how different factors affect the mechanism of SAGA-mediated nucleosome acetylation, we developed a bead-based, initial rate, steady-state nucleosome acetylation assay that extends our previously described acetylation sequencing assay (36). In our new assay, we immobilized biotinylated nucleosome GBY (Fig. 1A) onto streptavidin-coated magnetic beads. GBY was assembled from recombinant histones and a DNA template containing 147 bp of the 601 strong octamer positioning sequence that was flanked by 95 bp on one side and 15 bp on the other side. Embedded in the 95-bp flanking DNA and 24 bp away from the 147-bp sequence was a 17-bp recognition sequence for the yeast Gal4 transcriptional activator domain (37), although no activator protein was present in our initial assays. To perform the initial rate, steady-state assays, tritium-labeled acetyl-CoA, and purified native yeast SAGA complex were added to the bead-bound GBY nucleosomes, and aliquots of the reaction were removed at specific time points (Fig. 1A). These aliquots were washed to remove unincorporated acetyl-CoA and then counted by liquid scintillation.

These assays included concentrations of SAGA and nucleosomes that were significantly lower than we used previously (36) and required optimization to obtain greater sensitivity. Therefore, prior to counting samples by liquid scintillation, aliquots were washed with hydroxylamine to remove unincorporated acetyl-CoA. This compound cleaves the thioester bond of acetyl-CoA (38) and thereby liberates the tritiated acetyl group away from any CoA nonspecifically associated with the beads. Using this strategy, we found that linear rates of acetylation could be collected over a wide range of nucleosome concentrations, indicating that steady-state, initial rate kinetic analysis was possible. By plotting the initial rates of nucleosome acetylation as a function of nucleosome concentration (Fig. 1B), we observed saturation of acetylation activity on GBY nucle-

somes that was well fit to the Michaelis-Menten equation, yielding a K_m of 22 ± 4 nM and a k_{cat} of 1.0 ± 0.1 min⁻¹.

Additional experiments were next performed to interpret these kinetic constants. Although the K_m value of an enzyme is often used as shorthand for the dissociation constant (K_D) and for its substrate, there can be a significant deviation between the two. Formally, the K_m value represents the overall dissociation constant of all enzyme-bound species and can differ from the K_D value because of additional bound intermediates or rapid turnover. To determine the K_D value of SAGA for GBY nucleosomes, a binding titration, was performed between SAGA and the GBY nucleosomes in the presence of CoA via electrophoretic mobility shift assays (EMSA) (Fig. 1C). CoA was used in this assay because acetyl-CoA would result in turnover by the enzyme, potentially obfuscating our analysis of shifted nucleosome. In this experiment, the band corresponding to GBY nucleosome alone (Fig. 1C, left lane) decreases with increasing amounts of SAGA complex, concomitant with the appearance of a species with decreased mobility. The shifted species requires SAGA but is not SAGA alone as the DNA stain does not detect SAGA without nucleosomes (Fig. 1C, right-most lane). These results indicate formation of a complex between SAGA and the nucleosome and give a qualitative measurement of the strength of the interaction, where half-saturation of binding appears to occur at 16 ± 3 nM. This apparent K_D value is in rough agreement with the measured K_m of 22 nM, although it may reflect an increase in binding affinity between GBY nucleosome and SAGA.

To better understand the nature of the acetylation turnover parameter, k_{cat} , time-course experiments were done to probe early and late acetylation events. Initial experiments were performed with 200 nM nucleosome ($\sim 10 \times K_m$) at a concentration of SAGA complex close to nucleosome concentration (50 nM). Under these conditions, acetylation did not proceed with a simple linear or exponential rate (Fig. 1D). In the late time points, each nucleosome has been acetylated on average more than twice (for example, at 300 s each nucleosome has 10 acetylations on average). This indicates that this portion of the progress curve includes kinetic information on acetylation subsequent to the first histone acetylation. The rate in this region was significantly less than the rate of early time points, and one possible interpretation of these data is that after completing the first histone acetylation, subsequent acetylation is significantly slower. However, the rate of acetylation in the early time points is significantly greater than the measured steady-state turnover from the earlier experiment (Fig. 1B). This suggests that the reaction may undergo burst-phase kinetics, where the rate of pre-steady-state acetylation is faster than steady-state acetylation. To investigate this possibility, time-course experiments were repeated with less SAGA (4.5 nM), where acetylation of the first nucleosomal lysine would not proceed to completion. Under these conditions (Fig. 1E), as expected, nucleosome acetylation only proceeds to a limited extent (on average, only 4% of nucleosomes contained a single acetylation). However, the initial rates of acetylation still appear faster than the linear steady-state rate observed later in the time course, consistent with burst-phase kinetics. Thus, these

SAGA-mediated nucleosome acetylation

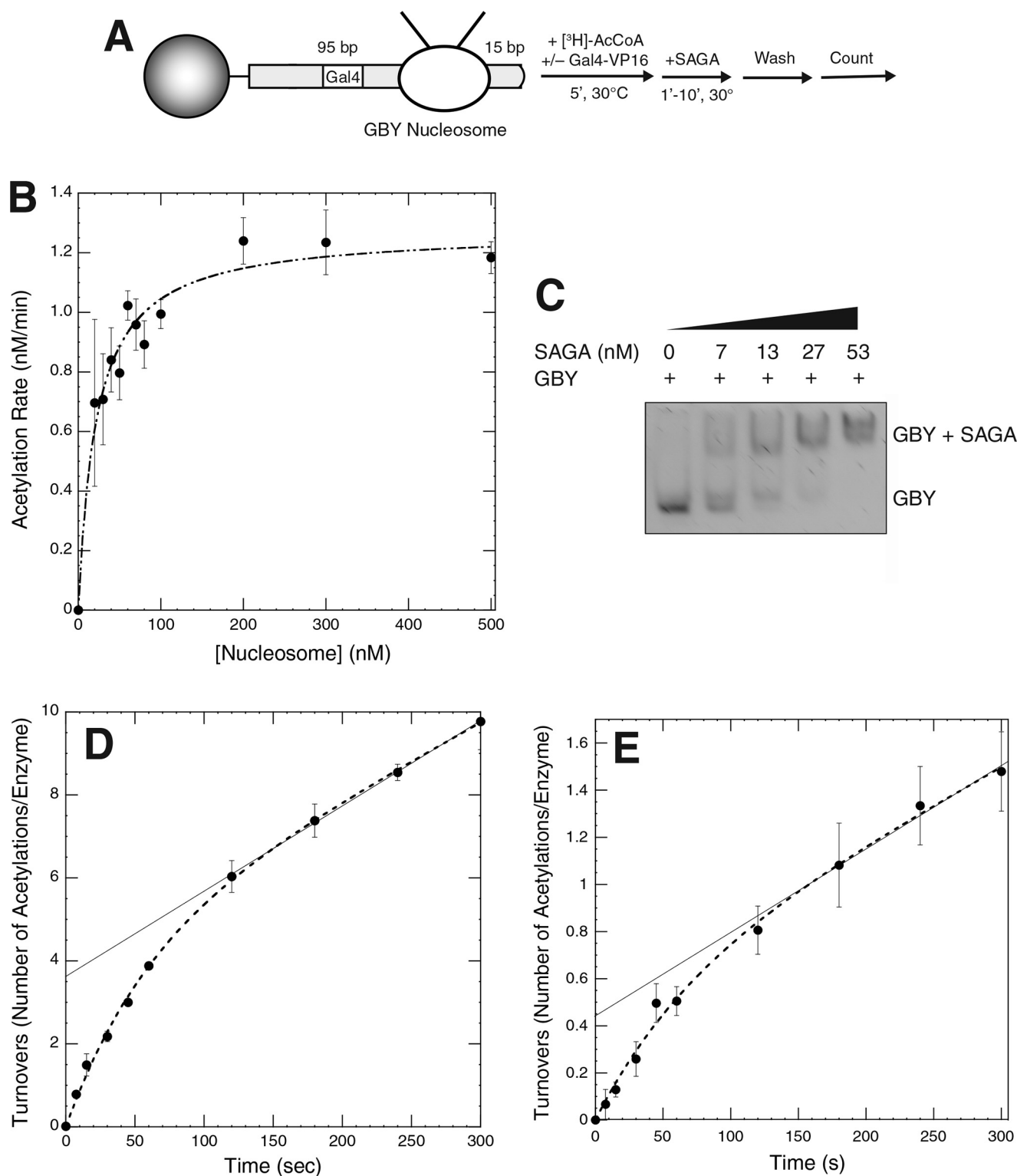


Figure 1. Characterization of SAGA nucleosome acetylation activity. *A*, schematic of the bead-bound GBY nucleosome and the steady-state nucleosome acetylation assay. GBY nucleosome stands for Gal body nucleosome and indicates that the nucleosome contains a Gal4-binding site in the body of the DNA, although initial assays were not performed with activator proteins. *B*, steady-state kinetics of GBY nucleosome acetylation. Initial rates of SAGA-mediated nucleosome acetylation were plotted at varying GBY nucleosome concentrations, and data were fit to the Michaelis-Menten equation. SAGA concentration was 1.25 nM. Error bars here and throughout represent the standard deviation of at least three trials. *C*, SAGA complex binds GBY nucleosomes with a high apparent affinity. EMSA was done with GBY nucleosomes and increasing amounts of SAGA complex. *D*, time course of SAGA-mediated nucleosome acetylation under saturating nucleosome-binding conditions with near-stoichiometric amounts of SAGA. Time-point data were fit to the sum of an exponential and linear component. To accentuate the difference between the early and late acetylation kinetics, a linear fit to a later portion of the time course is shown extrapolated to time 0. *E*, time course of SAGA-mediated nucleosome acetylation under saturating nucleosome-binding conditions with limiting amounts of SAGA. Data and fitting are treated similarly to *D*.

data together suggest that rapid acetylation proceeds steady-state acetylation turnover.

Effect of flanking DNA

To probe the effect of flanking DNA on nucleosome acetylation, we compared the GBY nucleosome (+95/+15) with a 147-bp nucleosome (+0/+0). This nucleosome is composed of the same recombinant histone proteins and 147 bp of the 601 strong positioning sequence as the GBY nucleosome with no flanking DNA. We found that in the absence of flanking DNA, the overall rate of nucleosome acetylation was reduced more than 5-fold (Fig. 2A), suggesting that flanking DNA stimulates nucleosome acetylation. Although our previous studies with GBY nucleosomes were not affected by attachment to the bead (36), we compared the rate of acetylation on bead-bound 147-bp nucleosomes to those free in solution to ensure this attachment was not responsible for the decreased activity (Fig. 2A). Attachment of the 147-bp nucleosome to the bead did not decrease the extent of its acetylation, confirming that reduction in 147-bp nucleosome acetylation relative to the GBY nucleosome was due to its lack of flanking DNA.

To characterize the mechanism by which flanking DNA stimulates nucleosome acetylation, we performed initial rate, steady-state kinetic analysis on the 147-bp nucleosome and compared the results with that of the GBY nucleosome (Fig. 2B). We found that without the flanking DNA, the rate of acetylation was lower at all nucleosome concentrations. Under saturating nucleosome concentrations, the rate of acetylation decreased 4-fold, corresponding to an equivalent decrease in k_{cat} (Table 1). Additionally, for the 147-bp nucleosome, the half-saturation of this activity required a greater nucleosome concentration, corresponding to an increase in K_m of 2.3-fold (Table 1). Thus, flanking DNA appears to stimulate nucleosome acetylation in two different ways, both by changing the K_m and k_{cat} values for the reaction, resulting in a 9.20-fold change of the selectivity constant of the reaction (k_{cat}/K_m).

To characterize the meaning of the K_m change, we again performed an EMSA experiment (Fig. 2C). In comparing the GBY and the 147-bp nucleosome, we found that the 147-bp nucleosome had a reduced apparent affinity for SAGA of 52 ± 12 nM, requiring 3.3 times the SAGA concentration to obtain the same degree of gel shift. Thus, this result supports the idea that underlying the ability of flanking DNA to change the K_m value of SAGA-mediated acetylation is an increased binding affinity for such nucleosomes, although the effect of flanking DNA on SAGA binding may be larger than its effect on the overall K_m of the reaction.

To help characterize the observed k_{cat} change, we performed an acetylation time course on the 147-bp nucleosome under near-saturating concentrations of nucleosomes (Fig. 2D). Like the GBY nucleosome, the 147-bp nucleosome exhibits a rapid rise in nucleosome acetylation followed by a slower, linear steady-state phase. However, both phases are significantly slower than those exhibited for the GBY nucleosome. Specifically, it appears that the rate of SAGA on the 147-bp nucleosome is four times slower than the GBY nucleosome at all time points, within the error of our measurements (Fig. 2E). This is in good agreement with the difference in k_{cat} values obtained

above (Fig. 2B), where the k_{cat} value of the GBY nucleosome was 4-fold faster than that for the 147-bp nucleosome and suggests that the flanking DNA stimulates multiple phases of nucleosome acetylation.

To determine which features of the flanking DNA stimulate SAGA-mediated acetylation, several different factors were investigated (all using 10 nM nucleosome and 2.0 nM SAGA). To probe whether the sequence or orientation of the flanking DNA were crucial, a GBY-like nucleosome was assembled such that the Gal4 consensus sequence was eliminated, and the flanking DNA orientation relative to the bead was flipped (+15/+95). The acetylation rate was then measured at a nonsaturating nucleosome concentration (20 nM) so that changes in either K_m and/or k_{cat} would be detected. The rate of acetylation of this nucleosome was slightly (1.3-fold) higher than that of the GBY nucleosome (Fig. 3A), indicating, at most, a modest role of sequence or nucleosome side in controlling acetylation rate.

To determine whether flanking DNA on both sides of the nucleosome stimulated acetylation, additional substrates were examined (Fig. 3B). A symmetric nucleosome with relatively limited amounts of flanking DNA (+15/+15) resulted in modest stimulation over nucleosomes lacking flanking DNA. However, a nucleosome with more flanking DNA (+80/+80) achieved stimulation similar to the GBY nucleosomes. To determine whether this stimulation required flanking DNA on both sides, nucleosomes with flanking DNA on a single side were examined (Fig. 3C). These nucleosomes were able to significantly stimulate acetylation. However, unlike the symmetric nucleosome with 80 bp on both sides (+80/+80), the nucleosome with 80 bp on a single side (+0/+80) did not show equivalent stimulation, indicating that DNA from both sides of the nucleosome contribute to stimulation.

The studies comparing SAGA binding to nucleosome with flanking DNA (GBY nucleosome) to those without (147-bp nucleosome) show that flanking DNA increases SAGA affinity (Fig. 2C). To probe how this increase occurs, binding to the flanking DNA alone was characterized (Fig. 3D). In these EMSA studies, the majority of DNA binding occurs with addition of 10 nM SAGA. This behavior is similar to the GBY nucleosome but dissimilar to the 147-bp nucleosome, and it suggests that the increase in SAGA binding to nucleosomes with flanking DNA occurs because SAGA can bind the DNA with higher affinity than to the nucleosome core itself.

Effect of activator protein

Because transcriptional activator proteins are known to interact with SAGA and facilitate targeted nucleosome acetylation (33, 35), we sought to quantify the magnitude and mechanism by which activators facilitate acetylation. For our studies, the fusion protein Gal4-VP16 (activator fusion protein containing a Gal4 activator DNA-binding domain and a VP16 activator activation region) was chosen as it is one of the best characterized activator protein systems and has been used extensively in studies of SAGA activity *in vivo* and *in vitro* (2, 34). Its interactions with other coactivators and general transcription factor complexes have also been well-studied (30–32). This protein contains the DNA-binding domain of the

SAGA-mediated nucleosome acetylation

yeast Gal4 activator and the activator domain of the herpes simplex virus protein, VP16 (39, 40).

Gal4-VP16 has been shown to bind to its consensus sequence with high affinity, and our EMSA experiments show

apparent low nanomolar affinity within the range of values reported in the literature (41–43). Utilizing recombinant Gal4-VP16 and the GBY DNA template used to make GBY nucleosomes, we showed that increasing amounts of activator

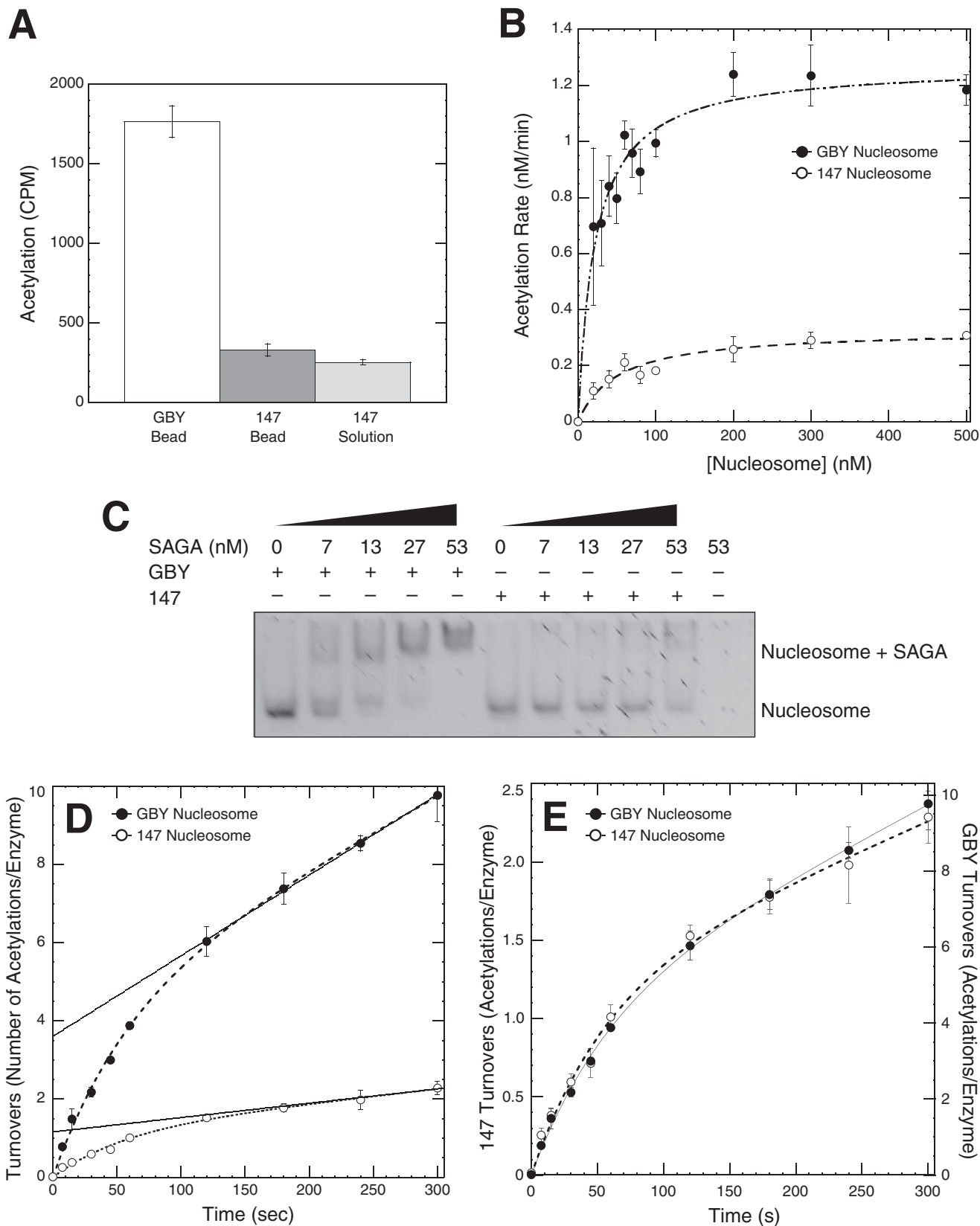


Table 1
Kinetic constants for SAGA-mediated nucleosome acetylation

Substrate	K_m	$k_{cat, app}$
	<i>nM</i>	<i>min⁻¹</i>
GBY nucleosome	22 ± 4	1.0 ± 0.1
147-bp nucleosome	50.6 ± 13.7	0.25 ± 0.02
GBY nucleosome + Gal4-VP16	46 ± 11	4.8 ± 1.1

protein resulted in formation of a shifted species with concomitant reduction of the free DNA (Fig. 4A).

Because these experiments indicate that the DNA-binding domain of the Gal4-VP16 is functional, we characterized to what extent the activator domain of Gal4-VP16 could stimulate acetylation. For these experiments, increasing amounts of Gal4-VP16 were titrated into reactions containing 20 nM GBY nucleosome and 2.5 nM SAGA (Fig. 4B). Nucleosome concentration was chosen to be nonsaturating so that potential stimulation of acetylation activity due to either changes in K_m and/or k_{cat} values would be observable. Indeed, strong activator-dependent stimulation of the acetylation rate was observed, which was especially apparent in comparing rates for high concentrations of activator (Fig. 4B, right points) versus those lacking activator (Fig. 4B, leftmost point). Furthermore, activator stimulation increased in a manner expected for saturation binding. At lower concentrations of Gal4-VP16, activator was sub-stoichiometric relative to nucleosomes, and stimulation was not complete. With more Gal4-VP16, stimulation increased up to a point. The observed plateau of stimulation at higher concentrations of activator, despite a stoichiometric excess of activator to nucleosome, presumably occurs because all Gal4-binding sites in the GBY nucleosomes are saturated.

To dissect how Gal4-VP16 mechanistically stimulates acetylation activity, we performed initial rate, steady-state nucleosome acetylation assays with varying concentrations of GBY nucleosome in the presence of a 2:1 ratio of activator/nucleosome (Fig. 4C). Our expectation had been that the activator would stabilize SAGA binding to nucleosomes, reducing the concentration of nucleosome required for half-saturation of acetylation activity (K_m) without changing SAGA acetylation activity when fully saturated with nucleosome (k_{cat}). However, that was clearly not the case. The presence of activator increased k_{cat} by 4.8-fold (Fig. 4C and Table 1). Additionally, the K_m value in the presence of activator was not decreased, but it increased from 22 ± 4 to 46 ± 11 nM (Fig. 4C and Table 1).

Because these reactions were initiated by SAGA addition and there could be an effect of slow binding of SAGA to activator, we modified our assay to initiate the reactions with acetyl-CoA after pre-incubation of SAGA with nucleosome and activator (Fig. 4D). Under these conditions, the rates of acetylation were comparable with our initial conditions, indicating that order of

addition was not a significant factor in the observed stimulation. Thus, our K_m and k_{cat} results suggest that activator works predominantly not by increasing the affinity of SAGA for nucleosome but by stimulating the turnover rate of acetylation.

To probe more directly the effect of activator on the binding of SAGA to nucleosome, EMSA experiments were performed on GBY nucleosomes with increasing amounts of SAGA, either with or without Gal4-VP16 (Fig. 4E). Unlike the case in which 147-bp nucleosomes changed the concentration of SAGA necessary to generate shifted species (Fig. 2C), the shifts with activator are not significantly different from those without. These data indicate that activator does not significantly increase the affinity constant of SAGA for nucleosome, consistent with the steady-state results.

To better characterize the source of the k_{cat} change, time-course experiments with activator protein were performed with saturating concentrations of nucleosomes. Direct comparison of the time courses for GBY nucleosome acetylation with and without Gal4-VP16 revealed that the presence of activator strongly augmented acetylation throughout the time course (Fig. 4F). As expected from our steady-state experiments, this increase included the later time points, corresponding to the steady-state phase of the reaction. This change was also observed in the early time points corresponding to the pre-steady-state phase. To a first approximation, this stimulation was relatively uniform throughout the time course, meaning that the activator largely affected the amplitude, but not its shape, as was observed for the time courses of nucleosomes with and without flanking DNA (Fig. 2E). That said, our data do show some differences in the shape of the time course in the steady-state region, where there appears to be a slight increase in the rate of acetylation. Nonetheless, even if present, the effect appears to be relatively modest.

To better understand Gal4-VP16-mediated stimulation, experiments were performed to probe which aspects of the activator were required. When increasing amounts of Gal4-VP16 are added to the 147-bp nucleosome, which lacks the Gal4-binding site, there is a significantly more modest stimulation of acetylation that does not reach the stimulation observed with the GBY nucleosome, even at significantly higher concentrations of activator protein (Fig. 5A, right). These data suggest that Gal4-VP16 by itself is less efficient in stimulating nucleosome acetylation if its DNA-binding site is not present. Follow-up experiments on the activator itself confirm the importance of both the DNA-binding and activator domains (Fig. 4B). BSA, a protein lacking both the DNA binding and activator domains, is unable to stimulate acetylation, showing that stimulation is not simply due to nonspecific interactions. Similarly, neither the VP16 activator domain alone nor the Gal4 DNA-

Figure 2. Effect of flanking DNA on SAGA activity. A, flanking DNA in the GBY nucleosome stimulates nucleosome acetylation activity. The extent of acetylation was measured for a bead-bound GBY nucleosome, a bead-bound 147-bp nucleosome lacking flanking DNA, and a 147-bp nucleosome free in solution (all with 1.5 nM SAGA and 52 nM nucleosomes). B, steady-state nucleosome acetylation analysis shows that the 147-bp nucleosome (white circles) has both an altered K_m and k_{cat} relative to the GBY nucleosome (black circles). Assays were performed as described in Fig. 1B, with data for the GBY nucleosome reproduced from Fig. 1B for comparison. C, lack of flanking DNA reduces the apparent affinity of SAGA for nucleosome. EMSA was done with GBY nucleosome (reproduced for comparison from Fig. 1C) or the 147-bp nucleosome, both with increasing amounts of SAGA complex. D, lack of flanking DNA reduces acetylation turnover at both initial and late acetylation. Experiments for the 147-bp nucleosomes (white circles) were performed as described for the GBY nucleosomes in Fig. 1D, with the GBY nucleosome data (black circles) included for comparison. E, flanking DNA uniformly affects the kinetics of initial and late nucleosome acetylation. Data from D are replotted, where the scale of the y axis for the 147-bp nucleosome (left axis) is shown at 4.12-fold that of the GBY nucleosome (right axis).

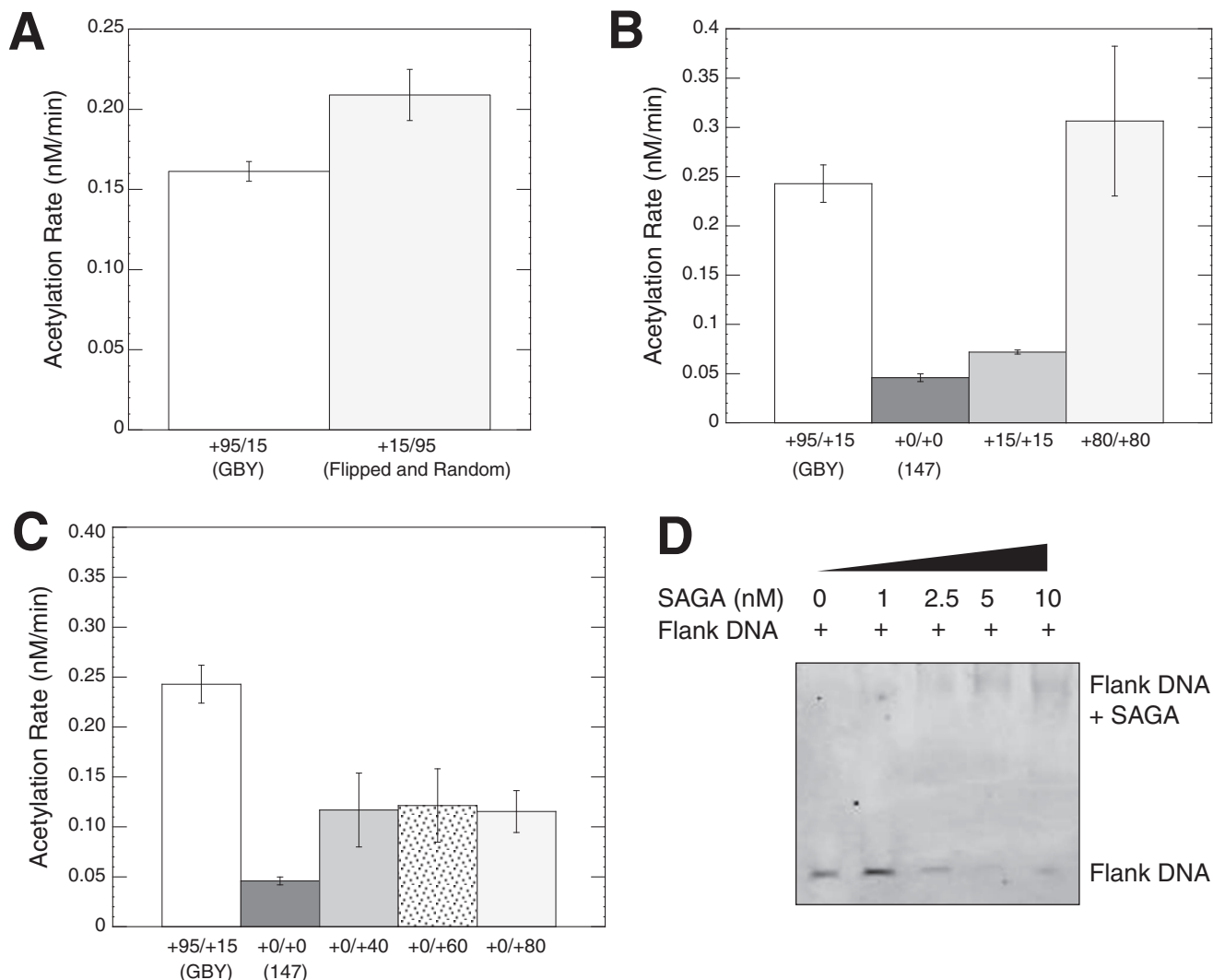


Figure 3. Characterization of flanking DNA requirements. *A*, sequence and orientation of flanking DNA with respect to the nucleosome do not change the rate of acetylation. Comparison of SAGA nucleosome acetylation activity between the GBY nucleosome (+95/+15) and one in which the flanking DNA has been flipped and the sequence randomized (+15/+95) is shown. *B*, flanking DNA larger than 15 bp on both sides of a nucleosome can fully stimulate acetylation. Comparison of SAGA nucleosome acetylation activity on GBY nucleosome, 147-bp nucleosome, and two nucleosomes that contain equal lengths of flanking DNA on both sides of the nucleosome (+15/+15 and +80/+80) is shown. *C*, flanking DNA on one side of the nucleosome increases acetylation but is not sufficient to stimulate full activity. Comparison of SAGA nucleosome acetylation activity on GBY nucleosome, 147-bp nucleosome (+0/+0), and three nucleosomes that contain differing amounts of flanking DNA only on one side of the nucleosome (+0/+40, +0/+60, and +0/+80) is shown. *D*, SAGA binds tightly to nucleosomal flanking DNA alone. EMSA with GBY flanking DNA with increasing amounts of SAGA complex is shown.

binding domain was able to stimulate acetylation, even at high concentrations.

Discussion

In this study, we have utilized nucleosome binding and acetylation assays to characterize how features of the environment surrounding nucleosomes affect acetylation. We find that both DNA flanking the nucleosome (+95/+15) and the presence of activator proteins significantly stimulate the rate of nucleosome acetylation, with each factor capable of increasing the rate of acetylation by 5-fold or more. We have determined some of the basic requirements for this stimulation. For the flanking DNA, DNA on both sides of the nucleosome could produce full stimulation, but full stimulation was not observed in the +15/+15 nucleosome (Fig. 3*B*). Thus, one side needs to more than 15 bp in length, whereas the other side can be 15 bp or less (Fig.

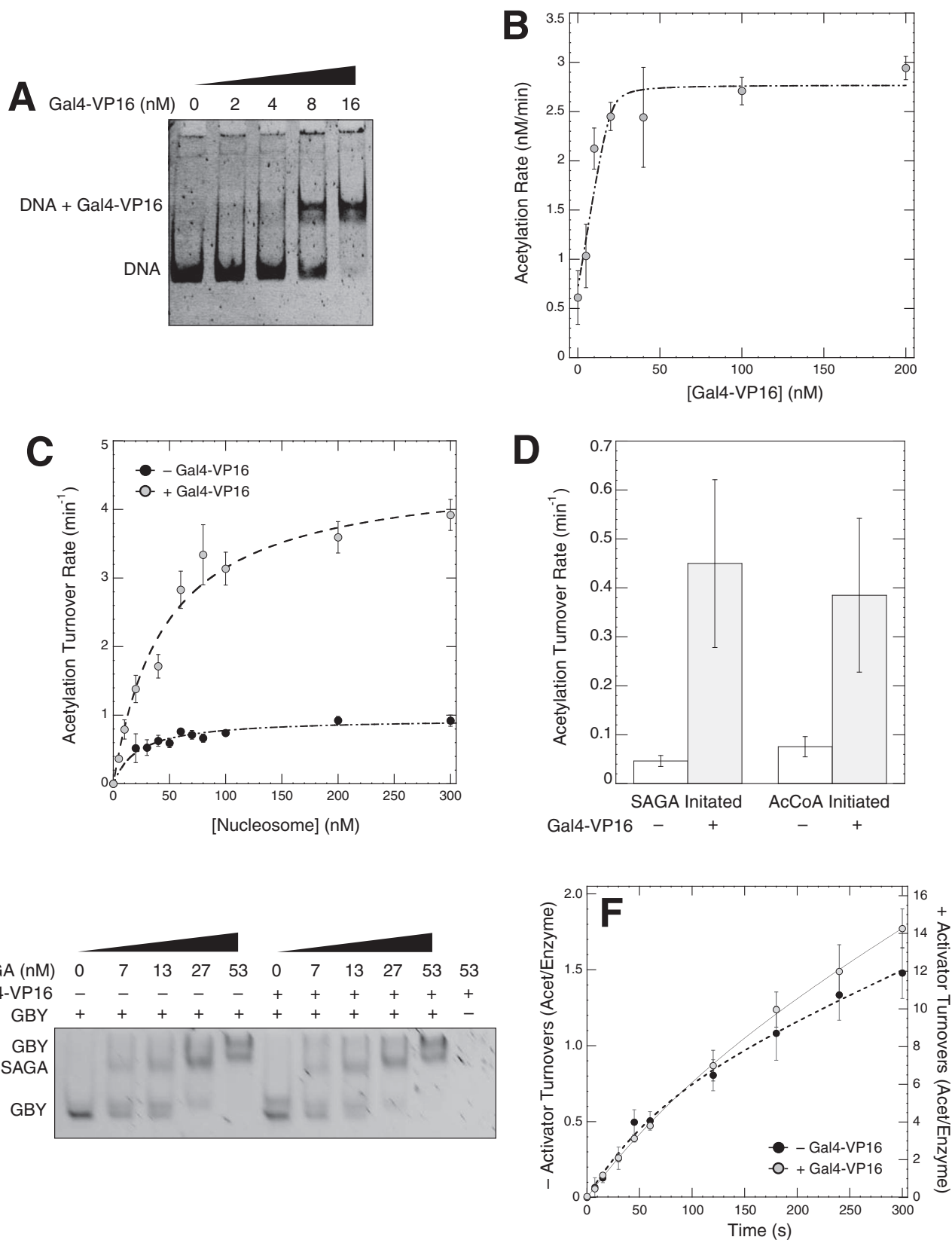
3*C*). For the activator, both domains together are necessary, and flanking DNA is required for full stimulation (Fig. 5, *A* and *B*). Together, these results suggest that activator directly stimulates acetylation via dual interaction with flanking DNA and SAGA.

Further kinetic analysis has allowed us to dissect mechanistic aspects of acetylation stimulation, and we observe two distinct mechanisms that contribute to a varying degree. One contributor is the changes in SAGA affinity for nucleosome. DNA flanking the nucleosome reduced the concentration of nucleosome necessary to achieve half-saturation of acetylation activity. Moreover, direct characterization of SAGA binding to nucleosome showed that the flanking DNA increases SAGA-binding affinity. In contrast, there does not appear to be a significant role of increased SAGA binding in activator-mediated stimulation, as neither the steady-state kinetic measurements nor

the direct nucleosome binding assays demonstrate improved SAGA binding in the presence of activator.

The other mechanism contributing to acetylation stimulation is an increase in the maximal steady-state rate of acetyla-

tion, and both flanking DNA and activator protein act through this mechanism. Further analysis shows that acetylation proceeds at distinct rates during different stages of the reaction and that flanking DNA and activator stimulate the rate of acetyla-



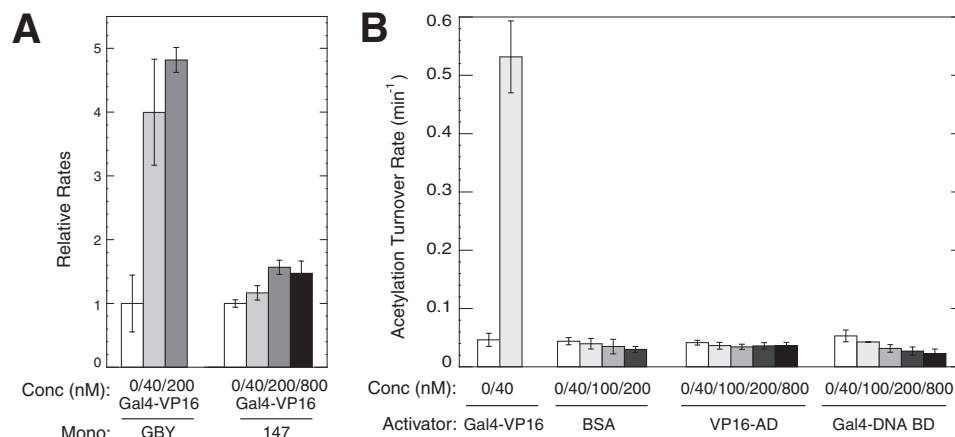


Figure 5. Characterization of activator requirements. A, full Gal4–VP16-mediated stimulation of nucleosome acetylation requires nucleosome flanking DNA. Comparison of initial acetylation rates for either GBY or 147-bp nucleosome with increasing amounts of Gal4–VP16 is shown. Acetylation rates have been normalized so that the rate without added protein is 1, and the data for the GBY nucleosome with Gal4–VP16 are the same as those shown in B. B, both the Gal4 DNA binding and VP16 activator domain are required for acetylation stimulation. Comparison of initial rates of GBY nucleosome acetylation with increasing amounts of bovine serum albumin (BSA), VP16 activator domain (VP16-AD), or Gal4 DNA-binding domain (Gal4-DNA BD) is shown.

tion at all stages. These stages include events after the first acetylation and before the first enzymatic turnover, where acetylation appears to proceed through a burst phase. It is possible that the observed changes in rates could simply be due to flanking DNA and activator increasing the affinity of SAGA for acetyl-CoA, such that stimulation would disappear with saturation of acetyl-CoA binding. However, this does not appear to be the case, as the extent of stimulation remains unchanged at high concentrations of acetyl-CoA ($10\times$ of K_m , data not shown).

The observation of burst-phase kinetics suggests potential mechanisms by which acetylation proceeds. In the basic model of burst-phase kinetics, the chemical step is fast relative to subsequent steps. This results in an initial burst of product, because the first time an enzyme acts it does so rapidly. However, to perform subsequent reactions, the enzyme has to proceed through the subsequent rate-limiting step, and consequently, the steady-state rate reflects the slower rate-limiting step. A common way that this can occur is through generation of a covalent intermediate during the reaction. This occurs, for example, in some proteases; a covalent adduct is formed between part of the peptide and the enzyme with rapid release of the other half of the peptide. At a much slower rate, a water molecule hydrolyzes the covalent enzyme–peptide intermediate, thereby releasing the peptide and enabling the enzyme to perform another catalytic cycle. Nucleosome acetylation could go through a covalent enzyme intermediate, where an acetyl group is transferred from acetyl-CoA to SAGA prior to transfer

of the acetyl group to the histone. However, prior studies with the catalytic Gcn5 subunit show that no covalent intermediate is formed (44). Furthermore, our assay specifically monitors generation of histone acetylation, not release of CoA, and does not retain SAGA on the beads (data not shown). Thus, it is unlikely that the observed burst-phase kinetics are due to a covalent enzyme intermediate.

Another common mechanism for burst-phase kinetics is that product release is slow relative to product generation. In this case, when product formation is monitored, there is a burst of product prior to the first turnover, with slower steady-state kinetics for subsequent turnovers. Our data are consistent with such a model where SAGA acetylation of the H3 histone could be relatively rapid, but the tight interactions of many subunits of SAGA with multiple parts of the nucleosome result in slow release of the acetylated nucleosome. This model is made more complicated by two additional factors. Because multiple sites of acetylation are available within the H3 histone and the nucleosome in general, this burst phase might additionally represent multiple histone acetylations prior to slow nucleosome release (16, 22). Also, because SAGA contains bromodomains that can bind acetylated histones, generation of nucleosome acetylation might itself promote SAGA retention, further slowing product release (45, 46). It should be noted that release and preferential rebinding of acetylated nucleosomes might mimic nucleosome acetylation without release. However, a published study is consistent with committed binding between multiple nucleosome acetylations (47), and thus we interpret the burst-phase kinetics

Figure 4. Effect of activator protein on SAGA activity. A, recombinant Gal4–VP16 protein binds tightly to DNA containing a Gal4 recognition site. EMSA with GBY nucleosome DNA and increasing amounts of Gal4–VP16 protein is shown. B, addition of Gal4–VP16 protein stimulates SAGA acetylation activity of a GBY nucleosome. The initial rate of nucleosome acetylation was assessed with varying concentrations of Gal4–VP16 dimer. The data were fit to a model of activator binding that takes into account the fact that Gal4–VP16 dimer was sub-stoichiometric relative to nucleosome at low activator concentrations. C, Gal4–VP16 protein stimulates SAGA acetylation activity by increasing k_{cat} . Comparison of the steady-state turnover (rate/enzyme) of GBY nucleosome acetylation in the presence (gray circles) or absence of Gal4–VP16 (black circles) is shown. The initial rate assays were performed as in Fig. 1B, and the data without Gal4–VP16 are reproduced for comparison. D, pre-incubation of SAGA with nucleosome and activator does not alter acetylation stimulation. Comparison of initial rates of GBY acetylation with and without Gal4–VP16 when reaction is either initiated with SAGA or acetyl-CoA addition. E, addition of Gal4–VP16 protein does not significantly change binding of SAGA to a GBY nucleosome. EMSA with GBY nucleosomes with or without Gal4–VP16 protein and with increasing amounts of SAGA is shown. F, addition of Gal4–VP16 stimulates both early and late phases of nucleosome acetylation (gray circles) compared with the same conditions without activator (black circles). The y axis for acetylation turnover in the presence of activator (right axis) has been significantly scaled down to directly compare the shape of the time course to the similar reaction without activator (left axis).

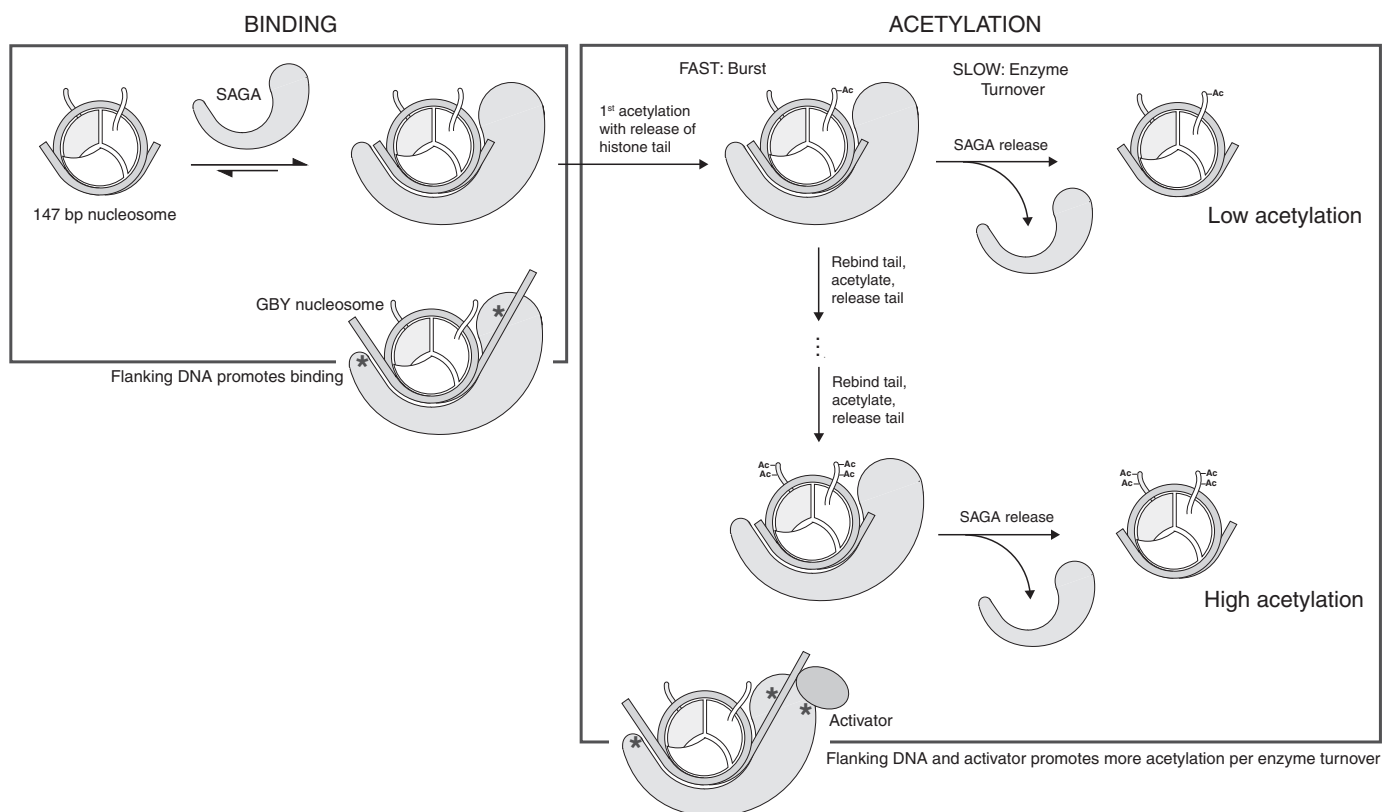


Figure 6. Possible model of nucleosome acetylation with role of flanking DNA and activator protein. Nucleosome acetylation proceeds through multiple steps, including nucleosome binding, H3 tail acetylation at multiple lysines without nucleosome release, and nucleosome release. Potential activating contacts between SAGA, flanking DNA, and activator are depicted with asterisks.

observed to being due to multiple acetylations prior to nucleosome release. Such a model (Fig. 6) provides a potential interpretation of how flanking DNA and activator can affect both the burst phase and steady-state phase of the reaction. If these factors facilitate more acetylation per turnover without changing the release rate, then increased acetylation would be observed both in the burst-phase first turnover and in higher levels of acetylation per turnover in the steady-state phase. How binding of DNA or activator increases acetylation per turnover is not clear but could occur through allosterically induced changes to the catalytic site.

The ability of DNA flanking the nucleosome to stimulate SAGA activity is not unique to this coactivator complex. ATP-dependent chromatin remodeling complexes have been shown to be influenced by nucleosome flanking DNA. For example, the chromatin-assembly factor complex spaces nucleosomes evenly on DNA by increasing its remodeling activity in response to longer flanking DNA (48). Additionally, the SWI/SNF-related (SWR1) complex incorporates the noncanonical histone H2A.Z/H2B dimer into the chromatin near nucleosome-free regions of DNA by preferentially binding and remodeling nucleosomes with flanking DNA (49). These examples demonstrate that flanking DNA is integral in the biological role of these chromatin remodeling complexes. Our results with SAGA suggest that the ability of the flanking DNA to change the localization and activity of chromatin remodeling complexes extends to those that modify histones, as well. Stimulation of SAGA binding and acetylation activity toward

nucleosomes possessing substantial flanking DNA may also contribute to its overall biological activity. The amount of flanking DNA surrounding a nucleosome varies throughout the genome. However, in budding yeast, the most common DNA distance between nucleosomes is 15 bp (50). This suggests that many nucleosomes would have less flanking DNA on both sides necessary for full SAGA activity, although our use of the strong 601–177–12 positioning sequence might have accentuated this effect by tightly sequestering the nucleosome entry–exit DNA that is more readily available for native nucleosomes. Changes in DNA–octamer interaction could extend to nucleosome positioning, where nucleosome density can decrease during transcription (51), and this could help facilitate SAGA action. For example, the SAGA complex is found at all open reading frames of all transcribed genes (21). As transcription occurs and nucleosome density decreases, SAGA might preferentially bind in these regions, acetylate nucleosomes, and promote downstream transcriptional events.

As the acetylation activity of SAGA is sensitive to flanking DNA, it is likely that subunits of SAGA directly bind to flanking DNA. Putative DNA-binding domains within subunits of SAGA have been identified and may serve this role. The *Swi3/Rsc9/Moir* (SWIRM) domain of mouse *Ada2 α* , a subunit required for the expanded specificity of *Gcn5* (22), was shown to bind dsDNA and a dinucleosome substrate with ~165 bp of linker DNA, but it does not bind a single nucleosome that lacks flanking DNA (52). Our activity results correspond with this observation, as SAGA demonstrates higher affinity and activity

on nucleosomes containing flanking DNA *versus* none. The zinc finger domain of Sgf11 is another putative DNA-binding domain in SAGA. Sgf11 associates with Ubp8, a subunit that performs the second catalytic activity of SAGA, the deubiquitination of histone H2B (53, 54). NMR titration experiments demonstrate that the zinc finger domain can weakly bind dsDNA but can strongly bind nucleosomes (55). However, this tight binding of nucleosomes may not result from DNA binding but from interaction of the domain with the acidic patch on the H2A/H2B dimer (56). Furthermore, both fission yeast and human TFIID have been shown to make interactions with the DNA beyond TATA-binding protein (TBP) interactions (57, 58). SAGA shares a core of TBP-associated factors with TFIID that act as a scaffold for assembly of other proteins, some of which may also interact with the DNA (59, 60).

Transcriptional activators bind to DNA consensus sequences and interact with coactivators and basal transcription factors to promote formation of the pre-initiation complex at promoters (61). SAGA has been shown to directly interact with a wide range of transcriptional activators (29), and the transcriptional activation domain of VP16 has been shown to interact with a number of SAGA subunits in isolation, including Ada2 (62, 63), Taf9 (64, 65), and Tra1 (29). However, cross-linking experiments with the full SAGA complex indicate that VP16 interaction occurs predominantly with the Tra1 subunit (29). The interaction of SAGA with activator results in localized nucleosome hyperacetylation *in vivo* at gene promoters and *in vitro* in reconstituted chromatin model systems (33, 34). Based on the ability of activators to bind coactivators and general transcription factors (30–32), the model generally proposed for activator function is that it recruits factors to the promoter. Indeed, in probing the source of activator-stimulated nucleosome acetylation (Fig. 4B), we expected that Gal4–VP16 would increase the affinity of SAGA for nucleosomes. On the contrary, our steady-state kinetic analysis of the saturation of acetylation activity (Fig. 4C) and direct characterization of nucleosome binding by SAGA (Fig. 4E) both indicate that activator does not increase binding affinity. Instead, activator appears to increase the overall acetylation turnover. Thus, our data suggest that at promoters, interaction of SAGA with activators does not act so much as to recruit SAGA but instead locally stimulates its acetylation activity. Such a model might predict that *in vivo* localization of SAGA is not enhanced by activator, which does not appear to be the case (35). However, because activator-enhanced nucleosome acetylation could also stabilize SAGA localization via direct acetylation binding and indirect access to the DNA (23), these pathways might also account for activator-enhanced SAGA localization.

This finding represents a novel mechanism of activator actions with respect to SAGA and potentially for activator-interacting proteins in general. Although it is not clear how interactions between Gal4–VP16 and SAGA produce this stimulation, based on the distance between the VP16-interacting subunit, Tra1, and the catalytic subunit, Gcn5 (60, 67), as mentioned above, it is possible that activator binding allosterically changes Gcn5 activity via some conformational change. Such allosteric activation by proteins is a common regulatory strategy, and even in the absence of activator there is evidence from

EM and cross-linking studies that SAGA, or SAGA missing specific subunits, can adopt different conformations (68–70). Additionally, the ability of activator proteins to induce conformational changes in binding partners has precedence. For example, the Rap1 activator protein can induce conformational changes in the basal transcription factor complex TFIIA (71), and various activators, including VP16, can induce conformational changes in the CRSP coactivator complex (72, 73).

From our studies, it is not clear how activator binding relates to stimulation from flanking DNA. In Fig. 4B, we observe that the Gal4-binding domain alone can reduce SAGA activity. This could be due to Gal4 binding precluding SAGA access to flanking DNA, thereby preventing such stimulation. However, because this effect requires relatively high concentrations of DNA-binding protein, there may also be effects outside of Gal4-binding site binding, such as nonspecific binding.

Experimental procedures

Nucleosome preparation

Biotinylated GBY DNA was prepared as described previously (36). All other DNA for nucleosome assembly were generated by PCR amplification using a forward primer containing a biotin moiety with a 15 atom spacer at the 5' end. DNA template details and sequences are provided in the [supporting Materials](#). Recombinant *Xenopus laevis* histones were prepared (74) and assembled into octamers, as described previously (75). Nucleosomes were assembled by depositing the histone octamer on different lengths of template DNAs by the process of rapid dilution and then dialysis into LDB buffer (2.5 mM NaCl, 10 mM Tris, pH 7.4, 0.25 mM EDTA), as described previously (76). The homogeneity and degree of saturation of the assembled nucleosomes were assessed on a 4% native PAGE and shown in Fig. S1. Nucleosomes were used without further purification. GBY nucleosome was immobilized on hydrophilic streptavidin beads from New England Biolabs, as described previously (36). Other nucleosomes containing biotinylated DNA were directly bound to the streptavidin beads by incubating ~200 µg of resin with 3.73 pmol of nucleosome at a final concentration of 150 nM.

SAGA and Gal4VP16 preparation

Endogenous SAGA complex from *Saccharomyces cerevisiae* was purified using the TAP purification strategy, as described previously (77). The purity of the complex was confirmed by silver stain gel analysis. The purified enzyme was quantitated by Western blotting compared with known amounts of recombinantly expressed and purified Gcn5 that had been quantified by Bradford analysis, and SAGA stocks were typically prepared at a concentration between 80 and 150 nM. Activity of the purified enzyme was assessed with a synthetic H3 peptide, as previously described (78). Recombinant Gal4VP16 was purified from *E. coli* Xa90 cells transformed with pJL2S plasmid (a generous gift from Dr. Steve Triezenberg) largely according to a previously published protocol (79).

Electrophoretic mobility shift assays

Binding between 2 nM GBY DNA and Gal4–VP16 (0, 2, 4, 8, 16, and 32 nM) was performed at room temperature for 15 min

in 20 μ l of binding buffer (10 mM HEPES, 100 mM NaCl, 5 mM DTT, 4 mM $\text{MgCl}_2 \cdot 6\text{H}_2\text{O}$, 1 mM PMSF, 5% glycerol, pH 7.5). Reaction products were resolved by 4% native PAGE at 60 V for 60 min in $0.5\times$ TBE. Binding between 5 nM GBY or 147-bp nucleosomes and SAGA (0, 7, 13, 27, and 53 nM) was performed at 30 °C for 9 min in a 7- μ l reaction. 5 nM nucleosomes were pre-incubated with 30 μ M CoA at 30 °C, with or without 20 nM Gal4–VP16. Reaction products were resolved on a pre-run (30 min at 100 V at 4 °C) composite gel (0.25% agarose and 2% acrylamide). The gel was run for 25 min at 100 V at 4 °C in $0.25\times$ TBE. Gels were stained with SYBR Gold stain. All EMSA experiments were performed at least two times.

Acetylation kinetics

Steady-state kinetics were performed under initial rate conditions, with limiting concentrations of SAGA (36). Generally, 25 μ l of bead-bound substrate at $2\times$ the desired final nucleosome concentration in LDB was mixed with 25 μ l of $2\times$ HAT buffer (50 mM Tris, pH 7.5, 10% glycerol, 0.25 mM EDTA, 300 mM NaCl, 2 mM DTT, 2 mM PMSF, 20 mM sodium butyrate, 8 μ M acetyl-CoA, with a specific activity of tritiated acetyl-CoA of 15.6–37.0 Ci/mmol). After incubating at 30 °C for 5 min, reactions were initiated by adding 1 μ l of SAGA stock (1.25–2.5 nM final enzyme). 10- μ l aliquots were taken at 0, 3, 6, and 9 min and were directly added to tubes containing 10 μ l of WB1 (100 mM NaCl, 50 mM Tris-Cl, 10 mM MgCl_2 , 1 mM DTT, 0.1% Triton X-100). Each sample was washed four times with WB1 at room temperature and five times with WB2 (50 mM NH_4OH , 0.1% Triton X-100, 50 mM Tris-Cl, pH 7.5) at 37 °C, with 25 min of incubation. The beads were resuspended in 10 μ l of WB1 and 6–9 ml of EcoScint scintillation mixture. Acetylation generated per time was determined from the counts/min by accounting for the specific activity of the labeled CoA, the instrument counting efficiency, counting efficiency of bead bound or solution substrate (same), reaction aliquot volume, counts/min to decays/min to curie conversion. Rates were fit to the Michaelis-Menten equation to get half-saturation and turnover parameters. Bead-free acetylation assays were performed as described previously (36). In all kinetic experiments, each condition was repeated at least three times.

Assays with a fixed concentration of nucleosome and increasing amounts of activator were performed as described above, but with 20 nM of either GBY or a 147-bp nucleosome and varying concentrations of Gal4–VP16 or BSA (0–800 nM). Data for increasing amounts of Gal4–VP16 with GBY nucleosome were fit to a quadratic form (80), to account for the fact that the concentration of activator was potentially close to its K_D value. For assays with increasing concentrations of nucleosome, Gal4–VP16 was added to $2\times$ the nucleosome, but otherwise performed as described above.

Experiments focused on characterizing the time course of more extensive acetylations were performed as above with either 4.5 or 50 nM SAGA and 200 nM nucleosome as above, but with an unlabeled acetyl-CoA reaction quench step. Specifically, 10- μ l reactions were stopped with the addition of 10 μ l of 250 μ M cold acetyl-CoA in WB1. In reactions containing Gal4–VP16 reactions, $2\times$ activator/GBY nucleosome was used. To fit a mechanism-free model of acetylation progression (81), acety-

lation incorporation was fit to the sum of a linear and simple exponential component. For a mechanism-based model of burst-phase kinetics, an analytically derived fit was utilized (66). To account for the possibility of multiple acetylations per enzyme turnover in the burst phase, the acetylations/turnover was included as a fit parameter.

Author contributions—C. M., S. J. C., and M. A. S.-K. conceptualization; C. M. and S. J. C. investigation; C. M. and S. J. C. writing-original draft; M. A. S.-K. writing-review and editing.

Acknowledgments—We thank Blaine Bartholomew and Steve Triezenberg for supplying Gal4–VP16 plasmids.

References

- Nagy, Z., and Tora, L. (2007) Distinct GCN5/PCAF-containing complexes function as co-activators and are involved in transcription factor and global histone acetylation. *Oncogene* **26**, 5341–5357 [CrossRef Medline](#)
- Berger, S. L., Piña, B., Silverman, N., Marcus, G. A., Agapite, J., Regier, J. L., Triezenberg, S. J., and Guarente, L. (1992) Genetic isolation of ADA2: a potential transcriptional adaptor required for function of certain acidic activation domains. *Cell* **70**, 251–265 [CrossRef Medline](#)
- Fassler, J. S., and Winston, F. (1988) Isolation and analysis of a novel class of Suppressor of Ty insertion mutations in *Saccharomyces cerevisiae*. *Genetics* **118**, 203–212 [Medline](#)
- Grant, P. A., Duggan, L., Côté, J., Roberts, S. M., Brownell, J. E., Candau, R., Ohba, R., Owen-Hughes, T., Allis, C. D., Winston, F., Berger, S. L., and Workman, J. L. (1997) Yeast Gcn5 functions in two multisubunit complexes to acetylate nucleosomal histones: characterization of an Ada complex and the SAGA (Spt/Ada) complex. *Genes Dev.* **11**, 1640–1650 [CrossRef Medline](#)
- Lee, K. K., Sardiu, M. E., Swanson, S. K., Gilmore, J. M., Torok, M., Grant, P. A., Florens, L., Workman, J. L., and Washburn, M. P. (2011) Combinatorial depletion analysis to assemble the network architecture of the SAGA and ADA chromatin remodeling complexes. *Mol. Syst. Biol.* **7**, 503 [Medline](#)
- Huisinga, K. L., and Pugh, B. F. (2004) A genome-wide housekeeping role for TFIID and a highly regulated stress-related role for SAGA in *Saccharomyces cerevisiae*. *Mol. Cell* **13**, 573–585 [CrossRef Medline](#)
- Spedale, G., Timmers, H. T., and Pijnappel, W. W. (2012) ATAC-king the complexity of SAGA during evolution. *Genes Dev.* **26**, 527–541 [CrossRef Medline](#)
- Xu, W., Edmondson, D. G., Evrard, Y. A., Wakamiya, M., Behringer, R. R., and Roth, S. Y. (2000) Loss of Gcn5l2 leads to increased apoptosis and mesodermal defects during mouse development. *Nat. Genet.* **26**, 229–232 [CrossRef Medline](#)
- McMahon, S. J., Pray-Grant, M. G., Schieltz, D., Yates, J. R., 3rd., and Grant, P. A. (2005) Polyglutamine-expanded spinocerebellar ataxia-7 protein disrupts normal SAGA and SLIK histone acetyltransferase activity. *Proc. Natl. Acad. Sci. U.S.A.* **102**, 8478–8482 [CrossRef Medline](#)
- Palhan, V. B., Chen, S., Peng, G. H., Tjernberg, A., Gamper, A. M., Fan, Y., Chait, B. T., La Spada, A. R., and Roeder, R. G. (2005) Polyglutamine-expanded ataxin-7 inhibits STAGA histone acetyltransferase activity to produce retinal degeneration. *Proc. Natl. Acad. Sci. U.S.A.* **102**, 8472–8477 [CrossRef Medline](#)
- García-Oliver, E., García-Molinero, V., and Rodríguez-Navarro, S. (2012) mRNA export and gene expression: the SAGA-TREX-2 connection. *Biochim. Biophys. Acta* **1819**, 555–565 [CrossRef Medline](#)
- Ghosh, S., and Pugh, B. F. (2011) Sequential recruitment of SAGA and TFIID in a genomic response to DNA damage in *Saccharomyces cerevisiae*. *Mol. Cell. Biol.* **31**, 190–202 [CrossRef Medline](#)
- Burgess, R. J., Zhou, H., Han, J., and Zhang, Z. (2010) A role for Gcn5 in replication-coupled nucleosome assembly. *Mol. Cell* **37**, 469–480 [CrossRef Medline](#)

14. Brownell, J. E., Zhou, J., Ranalli, T., Kobayashi, R., Edmondson, D. G., Roth, S. Y., and Allis, C. D. (1996) *Tetrahymena* histone acetyltransferase A: a homolog to yeast Gcn5p linking histone acetylation to gene activation. *Cell* **84**, 843–851 [CrossRef Medline](#)
15. Kuo, M. H., Brownell, J. E., Sobel, R. E., Ranalli, T. A., Cook, R. G., Edmondson, D. G., Roth, S. Y., and Allis, C. D. (1996) Transcription-linked acetylation by Gcn5p of histones H3 and H4 at specific lysines. *Nature* **383**, 269–272 [CrossRef Medline](#)
16. Grant, P. A., Eberharther, A., John, S., Cook, R. G., Turner, B. M., and Workman, J. L. (1999) Expanded lysine acetylation specificity of Gcn5 in native complexes. *J. Biol. Chem.* **274**, 5895–5900 [CrossRef Medline](#)
17. Guillemette, B., Drogaris, P., Lin, H. H., Armstrong, H., Hiragami-Hamada, K., Imhof, A., Bonneil, E., Thibault, P., Verreault, A., and Festenstein, R. J. (2011) H3 lysine 4 is acetylated at active gene promoters and is regulated by H3 lysine 4 methylation. *PLoS Genet.* **7**, e1001354 [CrossRef Medline](#)
18. Morris, S. A., Rao, B., Garcia, B. A., Hake, S. B., Diaz, R. L., Shabanowitz, J., Hunt, D. F., Allis, C. D., Lieb, J. D., and Strahl, B. D. (2007) Identification of histone H3 lysine 36 acetylation as a highly conserved histone modification. *J. Biol. Chem.* **282**, 7632–7640 [CrossRef Medline](#)
19. Katan-Khaykovich, Y., and Struhl, K. (2002) Dynamics of global histone acetylation and deacetylation *in vivo*: rapid restoration of normal histone acetylation status upon removal of activators and repressors. *Genes Dev.* **16**, 743–752 [CrossRef Medline](#)
20. Eberharther, A., and Becker, P. B. (2002) Histone acetylation: a switch between repressive and permissive chromatin. *EMBO J.* **3**, 224–229 [CrossRef](#)
21. Govind, C. K., Zhang, F., Qiu, H., Hofmeyer, K., and Hinnebusch, A. G. (2007) Gcn5 promotes acetylation, eviction, and methylation of nucleosomes in transcribed coding regions. *Mol. Cell* **25**, 31–42 [CrossRef Medline](#)
22. Balasubramanian, R., Pray-Grant, M. G., Selleck, W., Grant, P. A., and Tan, S. (2002) Role of the Ada2 and Ada3 transcriptional coactivators in histone acetylation. *J. Biol. Chem.* **277**, 7989–7995 [CrossRef Medline](#)
23. Hassan, A. H., Prochasson, P., Neely, K. E., Galasinski, S. C., Chandy, M., Carrozza, M. J., and Workman, J. L. (2002) Function and selectivity of bromodomains in anchoring chromatin modifying complexes to promoter nucleosomes. *Cell* **111**, 369–379 [CrossRef Medline](#)
24. Lo, W. S., Trievel, R. C., Rojas, J. R., Duggan, L., Hsu, J. Y., Allis, C. D., Marmorstein, R., and Berger, S. L. (2000) Phosphorylation of serine 10 in histone H3 is functionally linked *in vitro* and *in vivo* to Gcn5⁺ mediated acetylation at lysine 14. *Mol. Cell* **5**, 917–926 [CrossRef Medline](#)
25. Bian, C., Xu, C., Ruan, J., Lee, K. K., Burke, T. L., Tempel, W., Barsyte, D., Li, J., Wu, M., Zhou, B. O., Fleharty, B. E., Paulson, A., Allali-Hassani, A., Zhou, J. Q., Mer, G., *et al.* (2011) Sgf29 binds histone H3K4me2/3 and is required for SAGA complex recruitment and histone H3 acetylation. *EMBO J.* **30**, 2829–2842 [CrossRef Medline](#)
26. Laprade, L., Rose, D., and Winston, F. (2007) Characterization of new Spt3 and TATA-binding protein mutants of *Saccharomyces cerevisiae*: Spt3 TBP allele-specific interactions and bypass of Spt8. *Genetics* **177**, 2007–2017 [CrossRef Medline](#)
27. Sermwittayawong, D., and Tan, S. (2006) SAGA binds TBP via its Spt8 subunit in competition with DNA: implications for TBP recruitment. *EMBO J.* **25**, 3791–3800 [CrossRef Medline](#)
28. Sanz, A. B., Garcia, R., Rodriguez-Pena, J. M., Nombela, C., and Arroyo, J. (2016) Cooperation between SAGA and SWI/SNF complexes is required for efficient transcriptional responses regulated by the yeast MAPK Slt2. *Nucleic Acids Res.* **44**, 7159–7172 [CrossRef Medline](#)
29. Brown, C. E., Howe, L., Sousa, K., Alley, S. C., Carrozza, M. J., Tan, S., and Workman, J. L. (2001) Recruitment of HAT complexes by direct activator interactions with the ATM-related Tra1 subunit. *Science* **292**, 2333–2337 [CrossRef Medline](#)
30. Kobayashi, N., Boyer, T. G., and Berk, A. J. (1995) A class of activation domains interacts directly with TFIID and stimulates TFIID-TFIID-promoter complex assembly. *Mol. Cell. Biol.* **15**, 6465–6473 [CrossRef Medline](#)
31. Vojnic, E., Mourão, A., Seizl, M., Simon, B., Wenzek, L., Larivière, L., Baumli, S., Baumgart, K., Meisterernst, M., Sattler, M., and Cramer, P. (2011) Structure and VP16 binding of the Mediator Med25 activator interaction domain. *Nat. Struct. Mol. Biol.* **18**, 404–409 [CrossRef Medline](#)
32. Neely, K. E., Hassan, A. H., Wallberg, A. E., Steger, D. J., Cairns, B. R., Wright, A. P., and Workman, J. L. (1999) Activation domain-mediated targeting of the SWI/SNF complex to promoters stimulates transcription from nucleosome arrays. *Mol. Cell* **4**, 649–655 [CrossRef Medline](#)
33. Kuo, M. H., vom Baur, E., Struhl, K., and Allis, C. D. (2000) Gcn4 activator targets Gcn5 histone acetyltransferase to specific promoters independently of transcription. *Mol. Cell* **6**, 1309–1320 [CrossRef Medline](#)
34. Vignali, M., Steger, D. J., Neely, K. E., and Workman, J. L. (2000) Distribution of acetylated histones resulting from Gal4–VP16 recruitment of SAGA and NuA4 complexes. *EMBO J.* **19**, 2629–2640 [CrossRef Medline](#)
35. Bhaumik, S. R., and Green, M. R. (2001) SAGA is an essential *in vivo* target of the yeast acidic activator Gal4p. *Genes Dev.* **15**, 1935–1945 [CrossRef Medline](#)
36. Mittal, C., Blacketer, M. J., and Shogren-Knaak, M. A. (2014) Nucleosome acetylation sequencing to study the establishment of chromatin acetylation. *Anal. Biochem.* **457**, 51–58 [CrossRef Medline](#)
37. Giniger, E., Varnum, S. M., and Ptashne, M. (1985) Specific DNA binding of GAL4, a positive regulatory protein of yeast. *Cell* **40**, 767–774 [CrossRef Medline](#)
38. Stadtman, E. R. (1957) Preparation and assay of acyl coenzyme-A and other thiol esters—use of hydroxylamine. *Method Enzymol.* **3**, 931–941 [CrossRef](#)
39. Sadowski, I., Ma, J., Triezenberg, S., and Ptashne, M. (1988) GAL4-VP16 is an unusually potent transcriptional activator. *Nature* **335**, 563–564 [CrossRef Medline](#)
40. Triezenberg, S. (1995) Structure and function of transcriptional activation domains. *Curr. Opin. Genet. Dev.* **5**, 190–196 [CrossRef Medline](#)
41. Parthun, M. R., and Jaehning, J. A. (1990) Purification and characterization of the yeast transcriptional activator GAL4. *J. Biol. Chem.* **265**, 209–213 [Medline](#)
42. Liang, S. D., Marmorstein, R., Harrison, S. C., and Ptashne, M. (1996) DNA sequence preferences of GAL4 and PPR1: how a subset of Zn²⁺ Cys⁶ binuclear cluster proteins recognizes DNA. *Mol. Cell. Biol.* **16**, 3773–3780 [CrossRef Medline](#)
43. Hong, M., Fitzgerald, M. X., Harper, S., Luo, C., Speicher, D. W., and Marmorstein, R. (2008) Structural basis for dimerization in DNA recognition by Gal4. *Structure* **16**, 1019–1026 [CrossRef Medline](#)
44. Tanner, K. G., Langer, M. R., Kim, Y., and Denu, J. M. (2000) Kinetic mechanism of the histone acetyltransferase GCN5 from yeast. *J. Biol. Chem.* **275**, 22048–22055 [CrossRef Medline](#)
45. Dhalluin, C., Carlson, J. E., Zeng, L., He, C., Aggarwal, A. K., and Zhou, M. (1999) Structure and ligand of a histone acetyltransferase bromodomain. *Nature* **399**, 491–496 [CrossRef Medline](#)
46. Hassan, A. H., Awad, S., Al-Natour, Z., Othman, S., Mustafa, F., and Rizvi, T. A. (2007) Selective recognition of acetylated histones by bromodomains in transcriptional co-activators. *Biochem. J.* **402**, 125–133 [CrossRef Medline](#)
47. Ringel, A. E., Cieniewicz, A. M., Taverna, S. D., and Wolberger, C. (2015) Nucleosome competition reveals processive acetylation by the SAGA HAT module. *Proc. Natl. Acad. Sci. U.S.A.* **112**, E5461–E5470 [CrossRef Medline](#)
48. Yang, J. G., Madrid, T. S., Sevastopoulos, E., and Narlikar, G. J. (2006) The chromatin-remodeling enzyme ACF is an ATP-dependent DNA length sensor that regulates nucleosome spacing. *Nat. Struct. Mol. Biol.* **13**, 1078–1083 [CrossRef Medline](#)
49. Ranjan, A., Mizuguchi, G., FitzGerald, P. C., Wei, D., Wang, F., Huang, Y., Luk, E., Woodcock, C. L., and Wu, C. (2013) Nucleosome-free region dominates histone acetylation in targeting SWR1 to promoters for H2A.Z replacement. *Cell* **154**, 1232–1245 [CrossRef Medline](#)
50. Brogaard, K., Xi, L., Wang, J. P., and Widom, J. (2012) A map of nucleosome positions in yeast at base-pair resolution. *Nature* **486**, 496–501 [CrossRef Medline](#)
51. Adkins, M. W., Williams, S. K., Linger, J., and Tyler, J. K. (2007) Chromatin disassembly from the PHO5 promoter is essential for the recruitment of the general transcription machinery and coactivators. *Mol. Cell. Biol.* **27**, 6372–6382 [CrossRef Medline](#)

52. Qian, C., Zhang, Q., Li, S., Zeng, L., Walsh, M. J., and Zhou, M. M. (2005) Structure and chromosomal DNA binding of the SWIRM domain. *Nat. Struct. Mol. Biol.* **12**, 1078–1085 [CrossRef Medline](#)
53. Köhler, A., Zimmerman, E., Schneider, M., Hurt, E., and Zheng, N. (2010) Structural basis for assembly and activation of the heterotetrameric SAGA histone H2B deubiquitinase module. *Cell* **141**, 606–617 [CrossRef Medline](#)
54. Samara, N. L., Datta, A. B., Berndsen, C. E., Zhang, X., Yao, T., Cohen, R. E., and Wolberger, C. (2010) Structural insights into the assembly and function of the SAGA deubiquitinating module. *Science* **328**, 1025–1029 [CrossRef Medline](#)
55. Koehler, C., Bonnet, J., Stierle, M., Romier, C., Devys, D., and Kieffer, B. (2014) DNA binding by Sgf11 protein affects histone H2B deubiquitination by Spt-Ada-Gcn5-acetyltransferase (SAGA). *J. Biol. Chem.* **289**, 8989–8999 [CrossRef Medline](#)
56. Morgan, M. T., Haj-Yahya, M., Ringel, A. E., Bandi, P., Brik, A., and Wolberger, C. (2016) Structural basis for histone H2B deubiquitination by the SAGA DUB module. *Science* **351**, 725–728 [CrossRef Medline](#)
57. Elmlund, H., Baraznenok, V., Linder, T., Szilagy, Z., Rofougaran, R., Hofer, A., Hebert, H., Lindahl, M., and Gustafsson, C. M. (2009) Cryo-EM reveals promoter DNA binding and conformational flexibility of the general transcription factor TFIID. *Structure* **17**, 1442–1452 [CrossRef Medline](#)
58. Cianfrocco, M. A., Kassavetis, G. A., Grob, P., Fang, J., Juven-Gershon, T., Kadonaga, J. T., and Nogales, E. (2013) Human TFIID binds to core promoter DNA in a reorganized structural state. *Cell* **152**, 120–131 [CrossRef Medline](#)
59. Bieniossek, C., Papai, G., Schaffitzel, C., Garzoni, F., Chaillet, M., Scheer, E., Papadopoulos, P., Tora, L., Schultz, P., and Berger, I. (2013) The architecture of human general transcription factor TFIID core complex. *Nature* **493**, 699–702 [CrossRef Medline](#)
60. Han, Y., Luo, J., Ranish, J., and Hahn, S. (2014) Architecture of the *Saccharomyces cerevisiae* SAGA transcription coactivator complex. *EMBO J.* **33**, 2534–2546 [CrossRef Medline](#)
61. Weake, V. M., and Workman, J. L. (2010) Inducible gene expression: diverse regulatory mechanisms. *Nat. Rev. Genet.* **11**, 426–437 [CrossRef Medline](#)
62. Silverman, N., Agapite, J., and Guarente, L. (1994) Yeast ADA2 protein binds to the VP16 protein activation domain and activates transcription. *Proc. Natl. Acad. Sci. U.S.A.* **91**, 11665–11668 [CrossRef Medline](#)
63. Barlev, N. A., Candau, R., Wang, L., Darpino, P., Silverman, N., and Berger, S. L. (1995) Characterization of physical interactions of the putative transcriptional adaptor, ADA2, with acidic activation domains and TATA-binding protein. *J. Biol. Chem.* **270**, 19337–19344 [CrossRef Medline](#)
64. Uesugi, M., Nyanguile, O., Lu, H., Levine, A. J., and Verdine, G. L. (1997) Induced α helix in the VP16 activation domain upon binding to a human TAF. *Science* **277**, 1310–1313 [CrossRef Medline](#)
65. Nedialkov, Y. A., and Triezenberg, S. J. (2004) Quantitative assessment of *in vitro* interactions implicates TATA-binding protein as a target of the VP16C transcriptional activation region. *Arch. Biochem. Biophys.* **425**, 77–86 [CrossRef Medline](#)
66. Fersht, A. (1999) *Structure and Mechanism in Protein Science: A Guide to Enzyme Catalysis and Protein Folding*, pp. 139–155. W. H. Freeman and Co., New York
67. Wu, P. Y., Ruhlmann, C., Winston, F., and Schultz, P. (2004) Molecular architecture of the *S. cerevisiae* SAGA complex. *Mol. Cell* **15**, 199–208 [CrossRef Medline](#)
68. Durand, A., Bonnet, J., Fournier, M., Chavant, V., and Schultz, P. (2014) Mapping the deubiquitination module within the SAGA complex. *Structure* **22**, 1553–1559 [CrossRef Medline](#)
69. Nguyen-Huynh, N. T., Sharov, G., Potel, C., Fichter, P., Trowitzsch, S., Berger, I., Lamour, V., Schultz, P., Potier, N., and Leize-Wagner, E. (2015) Chemical cross-linking and mass spectrometry to determine the subunit interaction network in a recombinant human SAGA HAT subcomplex. *Protein Sci.* **24**, 1232–1246 [CrossRef Medline](#)
70. Setiaputra, D., Ross, J. D., Lu, S., Cheng, D. T., Dong, M. Q., and Yip, C. K. (2015) Conformational flexibility and subunit arrangement of the modular yeast Spt-Ada-Gcn5 acetyltransferase complex. *J. Biol. Chem.* **290**, 10057–10070 [CrossRef Medline](#)
71. Papai, G., Tripathi, M. K., Ruhlmann, C., Layer, J. H., Weil, P. A., and Schultz, P. (2010) TFIIA and the transactivator Rap1 cooperate to commit TFIID for transcription initiation. *Nature* **465**, 956–960 [CrossRef Medline](#)
72. Taatjes, D. J., Näär, A. M., Andel, F., 3rd., Nogales, E., and Tjian, R. (2002) Structure, function, and activator-induced chromations of the CRSP co-activator. *Science* **295**, 1058–1062 [CrossRef Medline](#)
73. Tsai, K. L., Tomomori-Sato, C., Sato, S., Conaway, R. C., Conaway, J. W., and Asturias, F. J. (2014) Subunit architecture and functional modular rearrangements of the transcriptional mediator complex. *Cell* **157**, 1430–1444 [CrossRef Medline](#)
74. Luger, K., Rechsteiner, T. J., and Richmond, T. J. (1999) Expression and purification of recombinant histones and nucleosome reconstitution. *Methods Mol. Biol.* **119**, 1–16 [Medline](#)
75. Luger, K., Rechsteiner, T. J., and Richmond, T. J. (1999) Preparation of nucleosome core particle from recombinant histones. *Methods Enzymol.* **304**, 3–19 [CrossRef Medline](#)
76. Blacketer, M. J., Feely, S. J., and Shogren-Knaak, M. A. (2010) Nucleosome interactions and stability in an ordered nucleosome array model system. *J. Biol. Chem.* **285**, 34597–34607 [CrossRef Medline](#)
77. Wu, P. Y., and Winston, F. (2002) Analysis of Spt7 function in the *Saccharomyces cerevisiae* SAGA coactivator complex. *Mol. Cell. Biol.* **22**, 5367–5379 [CrossRef Medline](#)
78. Li, S., and Shogren-Knaak, M. A. (2008) Cross-talk between histone H3 tails produces cooperative nucleosome acetylation. *Proc. Natl. Acad. Sci. U.S.A.* **105**, 18243–18248 [CrossRef Medline](#)
79. Dechassa, M. L., Zhang, B., Horowitz-Scherer, R., Persinger, J., Woodcock, C. L., Peterson, C. L., and Bartholomew, B. (2008) Architecture of the SWI/SNF-nucleosome complex. *Mol. Cell. Biol.* **28**, 6010–6021 [CrossRef Medline](#)
80. Pollard, T. D. (2010) A guide to simple and informative binding assays. *Mol. Biol. Cell* **21**, 4061–4067 [CrossRef Medline](#)
81. Sassa, A., Beard, W. A., Shock, D. D., and Wilson, S. H. (2013) Steady-state, pre-steady-state, and single-turnover kinetic measurement for DNA glycosylase activity. *J. Vis. Exp.* e50695 [CrossRef Medline](#)